ISSN 1840-4855
e-ISSN 2233-0046

Original scientific article
http://dx.doi.org/10.70102/afts.2025.1833.442

AN ADAPTIVE MPC FOR ALTERNATE ARM MODULAR MULTILEVEL CONVERTER PV TIED GRID CONNECTED HVDC TRANSMISSION NETWORK

D. Lenine[1*], P. Sai Sampath Kumar[2], B. Venkatesh Reddy[3], K. Jagadeesh[4], P. Sesi Kiran[5], J. Surya Kumari[6]

[1]Department of EEE, RGM College Engineering & Technology, Nandyal, Andhra Pradesh, India. e-mail: lenine.eee@gmail.com, orcid: https://orcid.org/0000-0001-8816-1631
[2] Department of EEE, RGM College Engineering & Technology, Nandyal, Andhra Pradesh, India. e-mail: sammitsme@gmail.com, orcid: https://orcid.org/0000-0001-9015-8319
[3]Department of EEE, Sri Venkateswara College Engineering, Tirupati, Andhra Pradesh, India. e-mail: venkateshreddy.b@svce.edu.in, orcid: https://orcid.org/0000-0002-6827-8522
[4]Department of EEE, G. Pulla Reddy Engineering College, Kurnool, Andhra Pradesh, India. e-mail: svujagadeeshk@gmail.com, orcid: https://orcid.org/0000-0003-3365-3764
[5]Department of EEE, RGM College Engineering & Technology, Nandyal, Andhra Pradesh, India. e-mail: sesikiran1987@gmail.com, orcid: https://orcid.org/0000-0002-2676-9729
[6]Department of EEE, RGM College Engineering & Technology, Nandyal, Andhra Pradesh, India. e-mail: jdsk.23@gmail.com, orcid: https://orcid.org/0000-0003-4248-8684

Received: June 12, 2025; Revised: August 28, 2025; Accepted: September 23, 2025; Published: October 30, 2025

SUMMARY

The Modular Multilevel Converter (MMC) has emerged as the preferred architecture for integrating renewable energy power plants into the grid via undersea HVDC cables and HVDC overhead lines. However, to mitigate the significant power pulsations introduced by the single-phase AC–DC conversion in its arms, the MMC necessitates the use of large DC-link capacitors. To address these limitations, the Alternate Arm Converter (AAC) topology integrates MMC arms with Director Switches (DS), thereby reducing the required number of sub-modules, potentially by half, when compared to conventional MMC configurations. Furthermore, the AAC provides inherent DC fault-blocking capability, which is a critical feature for future DC grid applications. Model Predictive Control (MPC) is widely employed due to its flexibility in incorporating multiple control objectives within a unified cost function. Nonetheless, the extensive number of possible switching states in AAC results in substantial computational complexity, posing challenges for real-time control implementation. To alleviate this computational burden, this work proposes the development of machine learning (ML)-based controllers for AAC, leveraging training data generated through model predictive control (MPC) operation. The system architecture utilizes a solar photovoltaic (PV) array as the DC energy source, interfaced with the AC grid via the proposed AAC-based high-voltage direct current (HVDC) transmission link. In this study, an artificial neural network (ANN) is employed as the machine learning (ML) framework. The wellness of the proposed scheme is confirmed over a comprehensive simulation analysis that employs a detailed switching converter model.

Key words: *modular multilevel converter, alternate arm converter, model predictive control, machine learning, artificial neural network.*

INTRODUCTION

High-Voltage Alternating Current (HVAC) is converted by converters to High-Voltage Direct Current (HVDC) by converters to allow the power to be transferred and connected between AC and DC transmission networks with ease. For such applications, two main converter topologies are currently in use. As power systems continue to evolve due to the growing need for highly interconnected networks, system-level integration issues and the interpretability of new modular voltage source converter (VSC) topologies must be addressed in HVDC infrastructures [1]. Additionally, the proliferation of various distributed energy resources (DERs) and the rising global energy demand highlight modern architectures employing VSC and, more recently, modular multilevel converter (MMC) topologies [18], [3].

Among the various power electronic solutions, Modular Multilevel Converters (MMCs) have gained prominence due to their scalability, high efficiency, and superior harmonic performance [20]. In particular, the Alternate Arm Modular Multilevel Converter (ARM-MMC) topology offers a promising approach for achieving reduced switching losses and improved system dynamics. However, the control of such complex systems remains challenging, especially when integrating large-scale photovoltaic (PV) arrays with the grid through HVDC links [4], [5], [8], [22].

MPC's ability to handle multivariable systems with constraints in a predictive framework makes it particularly suited for managing the dynamic behavior of ARM-MMCs in PV-tied grid-connected HVDC networks [10]. Yet, conventional MPC methods often face limitations in adaptability under varying operating conditions such as fluctuations in solar generation, grid disturbances, and changes in system topology [6], [9], [10], [12].

It is known that voltage-sourced converter-based HVDC (VSC-HVDC) systems are a good way to integrate remote renewable energy sources with large AC networks, and among the high-power converter topologies, the Modular Multilevel Converter (MMC) has garnered a lot of research interest because of its unique benefits that make it ideal for VSC-HVDC applications [19], [7]. The rudimentary notions and working philosophies of the MMC have been the subject of numerous investigations. However, the architecture has several drawbacks, such as the need for numerous sub-modules, each of which contains hefty and cumbersome DC capacitors, increasing the system's physical footprint. As a result, MMC layouts are not as small as other high-power converter designs. Furthermore, DC faults cannot be blocked by MMCs based on chopper cells. Using full-bridge sub-modules, on the other hand, improves DC fault-blocking capabilities but almost doubles the number of semiconductor devices needed, raising the complexity and cost of the system.

The Alternate Arm Converter (AAC) was first introduced in 2010 [21], [11]. This innovative topology extends the capabilities of conventional voltage source converters (VSCs) by reducing the amount of required H-bridge cells, lowering total power losses, then providing inherent DC fault-handling capability. In the AAC architecture, the converter voltage is synthesized by stacking H-bridge cells connected to the DC bus, while each arm incorporates an IGBT-based director switch that governs the current path between the higher and lower arms. However, a key limitation of AAC is its higher power losses compared to traditional Modular Multilevel Converters (MMCs).

Recent research has proposed several advanced hybrid multilevel converter topologies, among which the Alternate Arm Modular Multilevel Converter (AA-MMC) has garnered significant attention [23], [13], [14], [16]. This topology exhibits several attributes that make it highly suitable for HVDC applications. The key advantages of AA-MMC include:

- A flexible and modular architecture,
- Low switching losses,
- DC fault tolerance, eliminating the need for large, high-rated AC/DC breakers in HVDC systems,
- Fewer sub-modules compared to conventional MMCs, and

- The ability to generate nearly sinusoidal, low-harmonic AC currents.

These characteristics position the AA-MMC as a highly promising and practical solution for HVDC transmission systems. Furthermore, the end-to-end HVDC transmission system developed in this study is fully compatible with existing multi-terminal DC (MTDC) grid configurations and MMC-based HVDC architectures [15], [17].

This is how the rest of the paper is structured. The Alternate Arm Converter's (AAC) mathematical modelling and operating concept are presented in Section II. The design and implementation of the controllers based on artificial neural networks (ANN) and model predictive control (MPC) are described in Section III. Results are presented in Section IV and concluded in Section V.

OPERATING PRINCIPLE AND MODELLING OF AAC

A. Operating Principle

The Alternate Arm Modular Multilevel Converter (ARM-MMC) represents an advanced evolution of the conventional MMC topology, specifically designed to optimize switching losses and enhance system efficiency in HVDC transmission. The ARM-MMC architecture integrates key operational features of traditional MMCs with alternating arm conduction patterns, enabling partial arm conduction and the use of lower-frequency switching techniques.

Structural Overview

The ARM-MMC consists of two arms per phase, namely upper and lower arms, with each arm composed of a series connection of submodules (SMs), typically based on half-bridge or full-bridge circuits. Each arm also incorporates a director switch and an arm inductor to facilitate alternate conduction patterns. Unlike standard MMCs, which operate with continuous arm conduction, the ARM-MMC conducts alternately during different parts of the fundamental AC cycle, significantly reducing the switching frequency and associated losses.

Operating Principle

The director switches control of this alternation by either bypassing the entire arm or allowing the submodules to contribute their voltage to the phase output. This operational strategy results in reduced arm current ripple, improved efficiency, and lower thermal stress on power electronic components.

The IGBT switches in each full-bridge sub-module (as depicted in Figure 1) operate in complementary pairs—specifically, S1 and S3, and S2 and S4. To avoid short-circuit conditions, switches S1 and S2, as well as S3 and S4, must never be simultaneously closed. The operating sequence of the sub-module depends on the current direction and the desired capacitor voltage management.

- When the sub-module is in current-receiving mode, the capacitor charges by triggering S1 and S4, at the same time S2 and S3 remain open-circuit.
- Conversely, the capacitor discharges when switches S3 and S2 are triggered, i.e, closed, and S1 and S4 remain open, allowing current to flow through the sub-module.
- If the current reverses direction, the control sequence adapts accordingly: the capacitor charges when switches S2 and S3 are triggered, ie, closed, and discharges when switches S4 and S1 are left closed with S3 and S2 remaining open.

This controlled switching strategy ensures precise capacitor voltage regulation and supports efficient arm voltage synthesis within the overall converter operation.

B. Modelling of AAC

Here, the half-bridge is utilized for the AAC's typical model. Ideal switches will be utilized in place of IGBTs to make modelling easier. Equation 1 represents the sub-module voltage V_{mi} to be expressed. Where 'i denotes the sub-module's count, Ni is allocated 1 or 0 based on whether the sub-module's capacitor is being bypassed or activated, and V_{ci} is the voltage across that capacitor.

$$V_{mi} = N_i * V_{ci} \quad (1)$$

Equation 2 can be used to compute the voltage across the capacitor, where C indicates the value of capacitance & im represents the current through the sub-module.

$$\frac{C(dV_{ci})}{dt} = N_i * i_m \quad (2)$$

We obtain the average model for both arms of the A phase by starting with "S," which is the number related to sub-modules in the stack. Applying a 120-degree phase shift to the A phase will yield it for the other phases. Equations 3 and 4 provide the voltage required for the upper and lower arms, respectively. In this equation, i_u and i_l represent the current passing via the upper and lower arms, respectively.

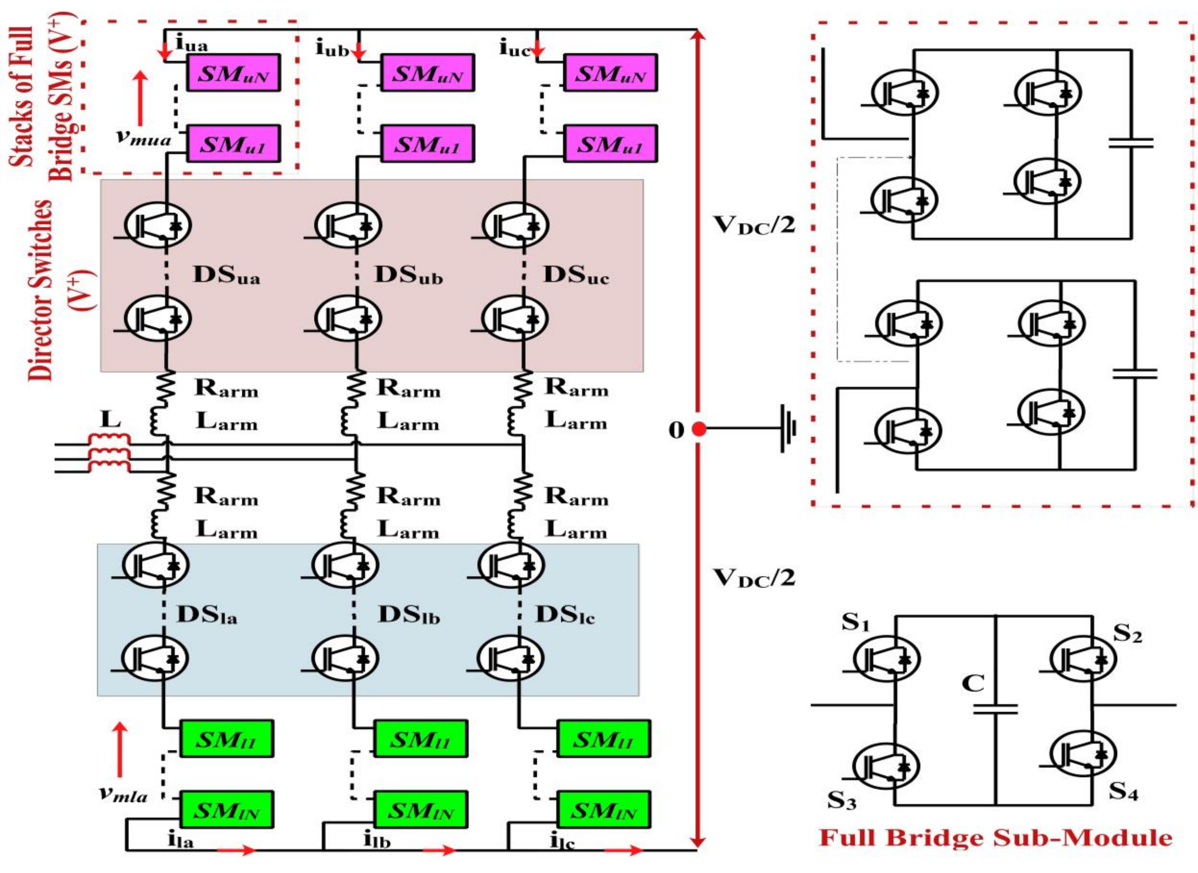

Figure 1. Structure of AAC

V_{lS} and V_{us} denote the capacitance voltages of the lower and upper arm of S number of sub-modules, respectively.

$$C\frac{(dV_{ls})}{dt} = N_s * i_l \quad (3)$$

$$C\frac{(dV_{us})}{dt} = N_s * i_u \quad (4)$$

Equations 5 and 6 can be used to express the cumulative voltage of the capacitors.

$$C\frac{d\sum_{i=1}^{S}V_{ls}}{dt} = \sum_{i=1}^{S} N_{li} * li \quad (5)$$

$$C\frac{d\sum_{i=1}^{S}V_{us}}{dt} = \sum_{i=1}^{S} N_{ui} * ui \quad (6)$$

By using KVL, we derive the current expressions from the upper and lower arms of phase A. Equations 7 and 8 show the current equations for the inductor.

$$L_l\frac{(di_l)}{dt} = {}^{V_{DC}}/_{2} + V_{ac} - R_l * i_l - V_{larm} \quad (7)$$

$$L_u\frac{(di_u)}{dt} = {}^{V_{DC}}/_{2} + V_{ac} - R_u * i_u - V_{uarm} \quad (8)$$

where V_{DC} denotes the DC voltage, L_l and L_u are the inductors representing lower and upper arms, respectively, R_l and R_u denote the resistances of lower and upper arms, respectively, V_{larm} and V_{uarm} specify the arm potential of lower and upper arm modules, and V_{ac} indicates the AC voltage.

IMPLEMENTATION OF THE ANN-BASED MPC CONTROLLER

A. MPC Control Algorithm

The standard MPC for AAC can be presented stage by stage as below, using 1 phase of the controller. The steps are as follows:

- Measuring input parameters of MPC
- Forecasting output and circulating current of each possible inserted sub-module for the upcoming sampling interval.
- Forming the cost equation using the information from the above currents.
- Choosing the appropriate upper or lower arm sub-module number that has the minimum value of cost.
- Applying the above chosen best arm in the module.

B. ANN Control Algorithm

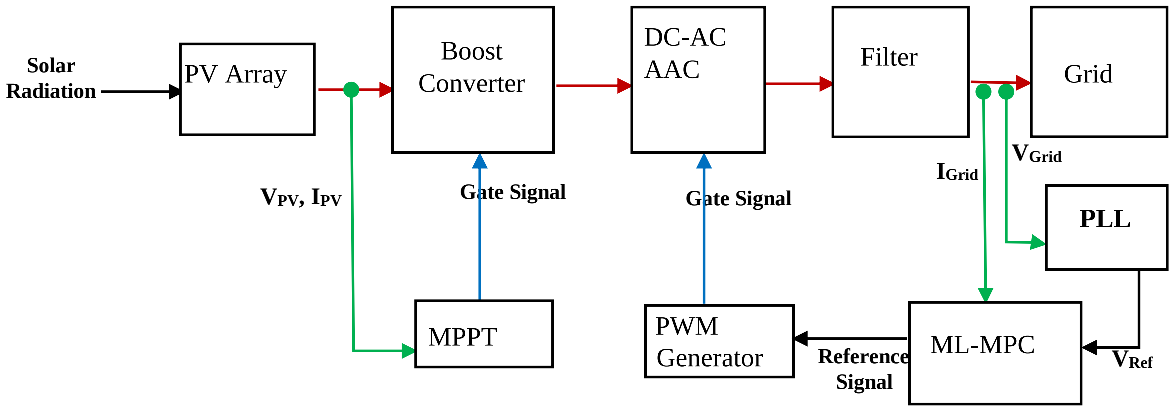

(a)

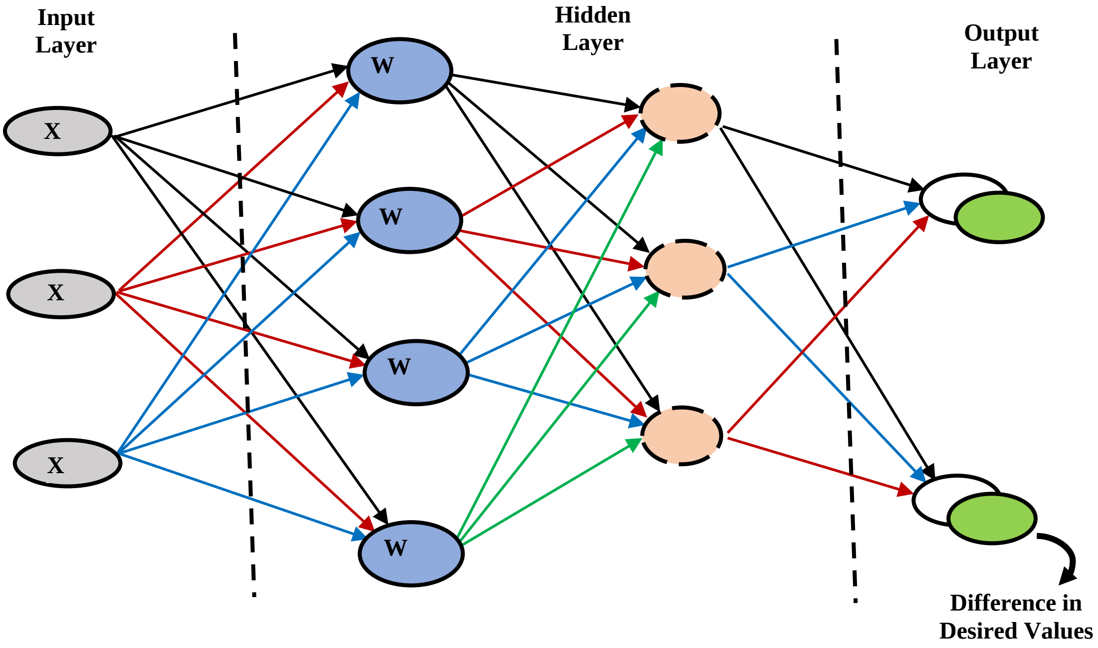

(b)

Figure 2. (a) Control structure of ANN-based MPC controller for AAC, (b) Structure of BP ANN

Figure 2a illustrates the implementation of the Machine Learning-based MPC controller block replacing the standard MPC controller, which can be directly connected to the Grid. A back-propagation (BP) type ANN method is utilized in this study, and its structure is presented in Figure 2b. The training data obtained by the MPC algorithm is used for the ANN training purposes. All of the steps in the training process are illustrated below for clarity [1][2].

- N data samples are produced by the MPC algorithm.

- The samples were randomly separated into three groups, namely, the training group, which utilizes 70% of the data, the validation group, which utilizes 15% of the data, and lastly, the testing group, which takes the remaining data. Once the ANNs have been trained by using the obtained data, they can be employed to determine the N_{ui} and N_{li} of AAC using a MATLAB Code in real time. The output of the network should normally be processed, which can be used to control the output current.

SIMULATION RESULTS AND DISCUSSIONS

The proposed ANN-based MPC controller for the AAC topology has been modeled and evaluated, and the simulation results are presented herein Table I.

Table 1. Parameters of simulation

Parameter	Value
Load Near AAC	10kW
Load Near Grid	5kW
Inductive Reactive Power	10kVAR
Battery Voltage	7kV
Battery Rating	3kAh

Figure 3 represents the waveforms of solar voltage, PV & IV curve, and its output power, respectively. Figure 4a and Figure 4b depict the current and comparison of actual and reference voltage waveforms of the converter output.

The 11 levels of the capacitor voltage for the lower sub-module have been presented in Figure 5a, and its corresponding average value is shown in Figure 5b.

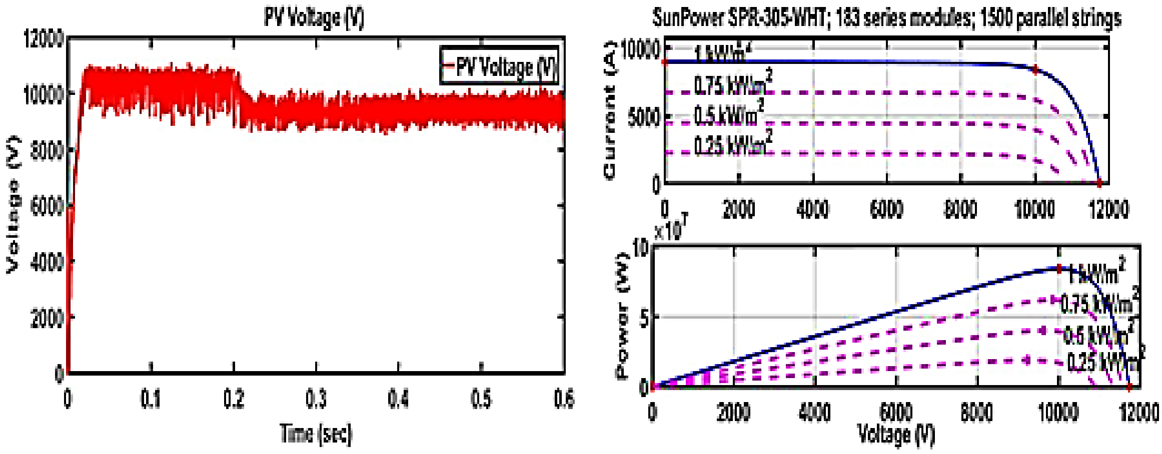

(a) (b)

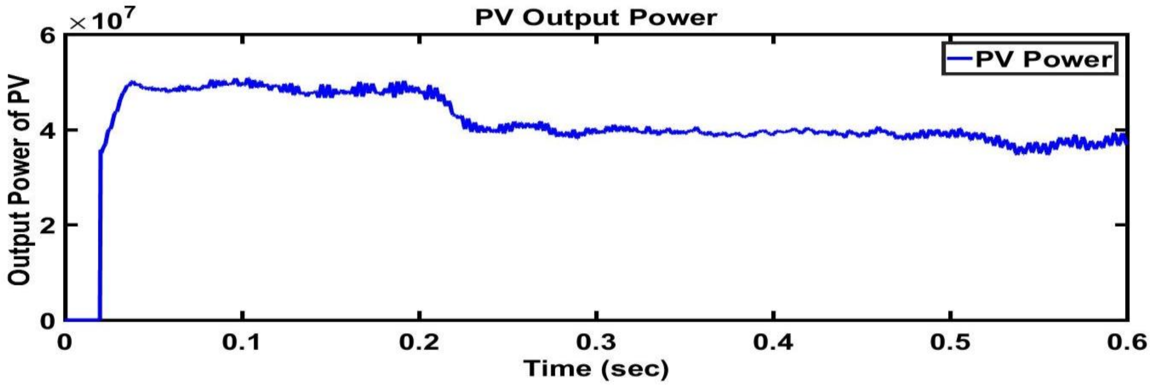

(c)

Figure 3. Solar Panels Outputs: (a) PV output voltage, (b) Solar IV & PV Curves, (c) output current with the Filter of the converter

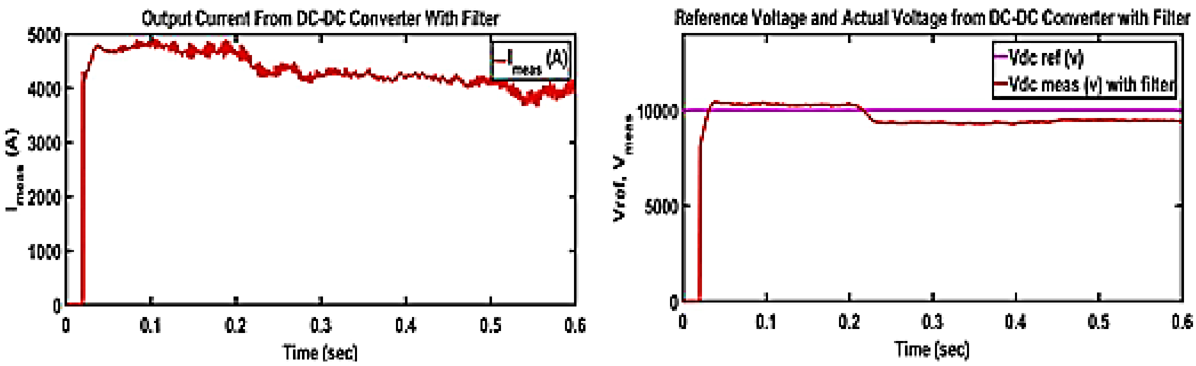

(a) (b)

Figure 4. Capacitor (a) output current with filter of converter (b) Actual Voltage vs Reference Voltage of Converter

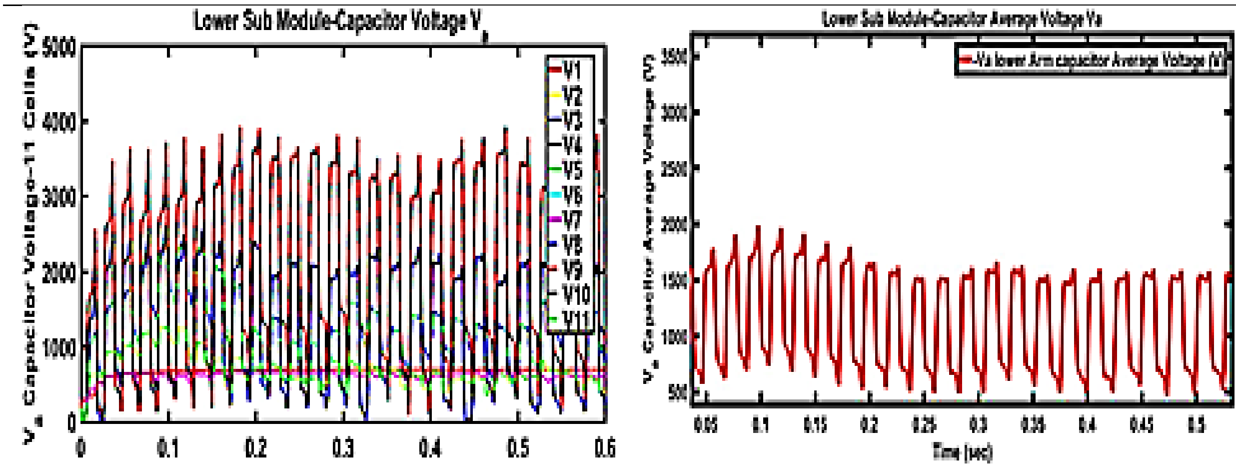

(a) (b)

Figure 5. Capacitor (a) Capacitor voltage for 11-cells (lower module) (b) Average capacitor voltage (lower module)

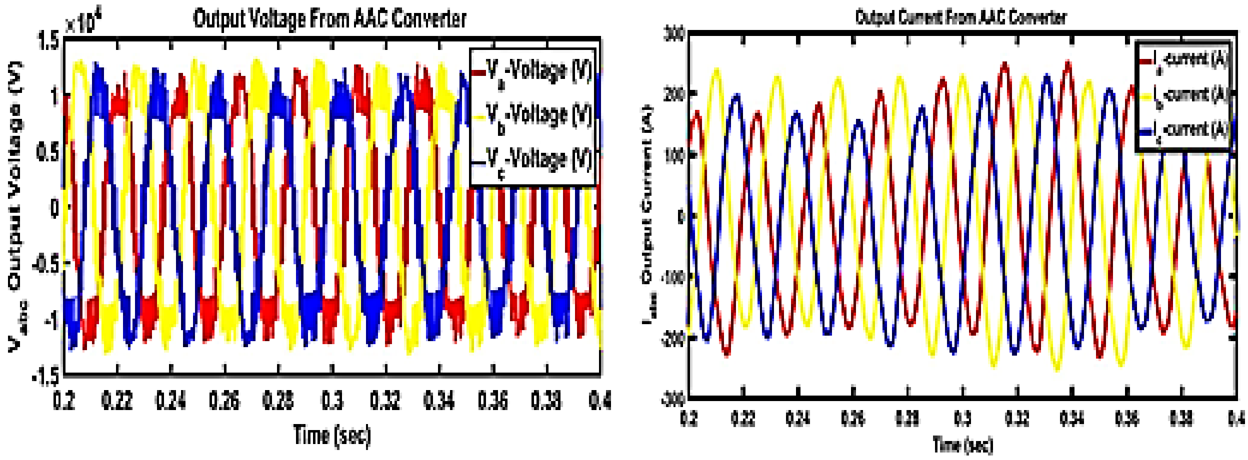

(a) (b)

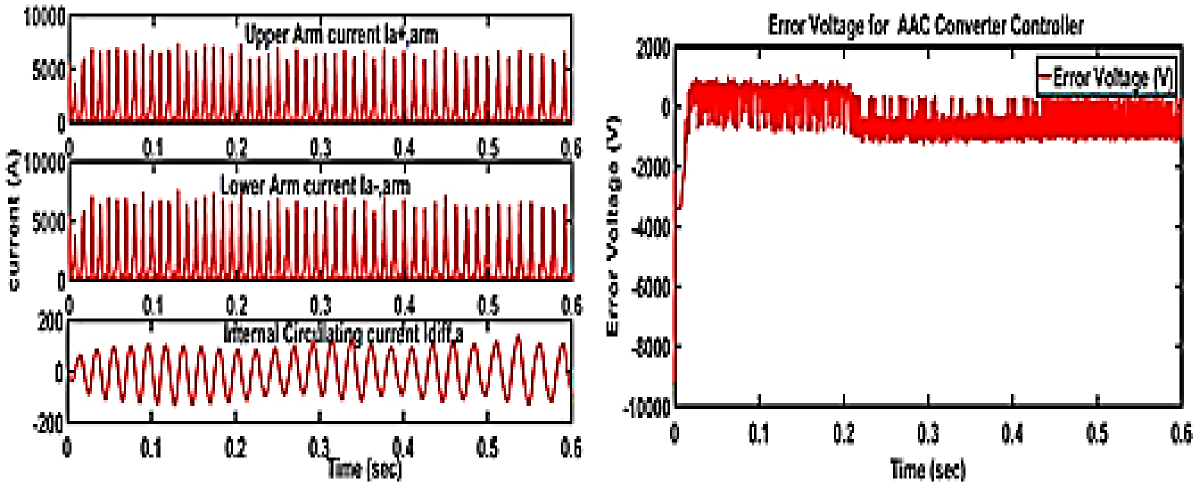

(c) (d)

Figure 6. AAC's (a) AAC's output voltage, (b) AAC's output current, (c) AAC's arm currents & circulating Current (d) AAC controller's error voltage.

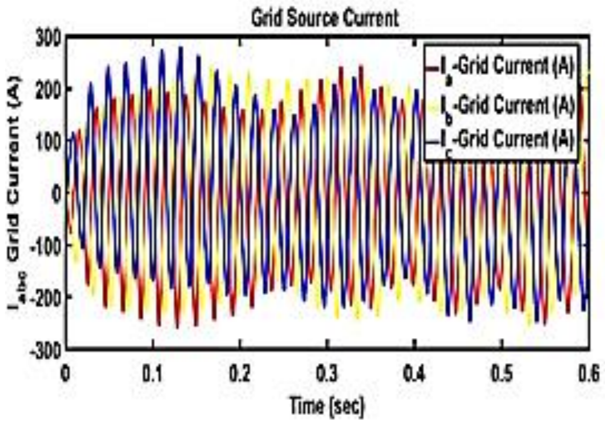

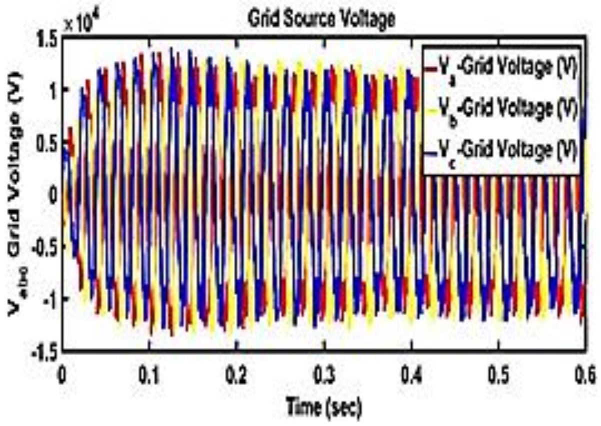

(a) (b)

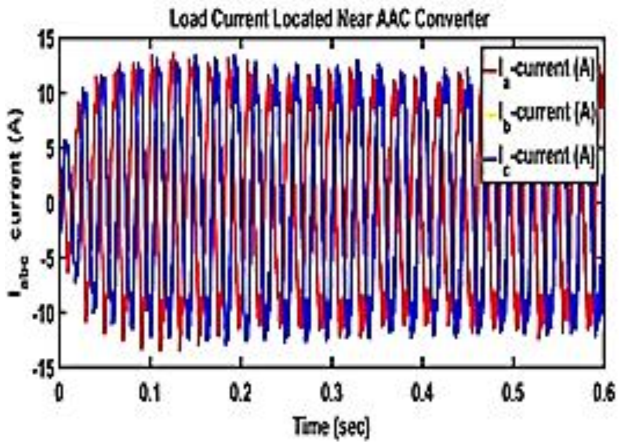

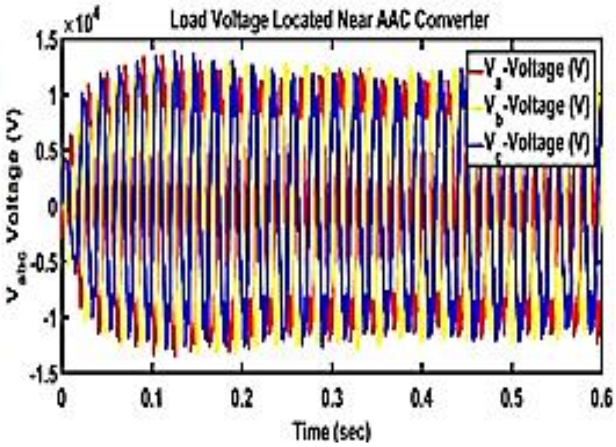

(c) (d)

Figure 7: Grid side and Load side voltage and current waveforms: (a) Current at Grid side, (b) Grid side voltage, (c) Current at Load side (d) Load side voltage

The AAC output current is shown in Figure 6(a), and the output voltage is shown in Figure 6(b); their corresponding current waveforms are presented in Figure 6(c). The voltage waveform regarding the error of the controller is shown in Figure 6(d). Additionally, Figure 7 presents the grid side and load side voltage and current.

CONCLUSION

This research proposes a novel ANN-based Model Predictive Control (MPC) strategy for a solar power grid-connected system employing an Alternate Arm Converter (AAC). The controller design and its performance have been validated through detailed simulation studies. Unlike the traditional MPC algorithm, which involves complex optimization computations, the trained ANN models rely solely on basic arithmetic operations, enabling a significant reduction in the real-time computational burden. These ANN-based models are effectively trained to replicate the behavior of MPC controllers. Theoretical analysis and simulation results demonstrate that the proposed AAC topology is well-suited for HVDC applications. Moreover, the ANN-based controller offers a compelling advantage over conventional MPC by substantially lowering the computational requirements, thereby facilitating more efficient and practical real-time control implementations.

ACKNOWLEDGMENT

The financial assistance of AICTE-RPS, New Delhi, File No. 8-198/ FDC/ RPS (SC-ST)/ POLICY-1/ 2021-22, is gratefully acknowledged by the author.

CONFLICT OF INTEREST

The authors declare no conflict of interest.

REFERENCES

[1] Wang S, Dragicevic T, Gao Y, Teodorescu R. Neural network based model predictive controllers for modular multilevel converters. IEEE Transactions on Energy Conversion. 2020;36(2):1562-1571. doi:10.1109/TEC.2020.3021022.

[2] Michael P, Jackson K. Advancing scientific discovery: A high performance computing architecture for AI and machine learning. Journal of Integrated VLSI, Embedded and Computing Technologies. 2025;2(2):18-26. https://doi.org/10.31838/JIVCT/02.02.03

[3] Zhou H, Yao W, Ai X, Li D, Wen J, Li C. Comprehensive review of commutation failure in HVDC transmission systems. Electric Power Systems Research. 2022; 205: 107768. https://doi.org/10.1016/j.epsr.2021.107768.s

[4] Bharathi C, Rekha D. Load Forecasting for Demand Side Management in Smart Grid using Non-Linear Machine Learning Technique. J. Wirel. Mob. Networks Ubiquitous Comput. Dependable Appl. 2023 Jul 20;14(1):200-14. https://doi.org/10.58346/JOWUA.2023.I1.016

[5] Rajan P, Jeevananthan S. A new partially isolated hybrid output of multiport multilevel converter for photovoltaic based power supplies. Journal of Energy Storage. 2022 Jan 1;45:103436. https://doi.org/10.1016/j.est.2021.103436

[6] Johanne M, Magnus A, Sofie I, Alexander H. IoT-based smart grid systems: New advancement on wireless sensor network integration. Journal of Wireless Sensor Networks and IoT. 2025;2(2):1-0.

[7] Kumar PS, Suresh P, Lenine D. Performance improvement of predictive voltage control for interlinking converters of integrated microgrid. Measurement: Sensors. 2024 Jun 1; 33: 101196. https://doi.org/10.1016/j.measen.2024.101196.

[8] Voralova E, Kreutzberg TH. Topology optimization for weight reduction in structural components under static loading. Association Journal of Interdisciplinary Technics in Engineering Mechanics. 2025;3(1):20-24.

[9] Kumari JS, Lenine D, Satish A, Kumar TS, Kalaivani C, Kumar MD, Rao YM. A model predictive Goertzel algorithm-based active islanding detection for grid-integrated photovoltaic systems. Microprocessors and Microsystems. 2022; 95: 104706. https://doi.org/10.1016/j.micpro.2022.104706.

[10] El Haj A, Nazari A. Optimizing renewable energy integration for power grid challenges to navigating. Innovative Reviews in Engineering and Science. 2025;3(2):23-34. https://doi.org/10.31838/INES/03.02.03

[11] Vasu M, Lenine D, Kumari JS, Kumar TS. Design and Analysis of Controller with Selective Harmonic Compensator for Grid Connected PV System. InE3S Web of Conferences 2021 (Vol. 309, p. 01009). EDP Sciences. https://doi.org/10.1051/e3sconf/202130901009

[12] Le VH. An optimal model for allocation readers with grid cell size and arbitrary workspace shapes in RFID network planning. Journal of Internet Services and Information Security. 2024;14(1):180-194. https://doi.org/10.58346/JISIS.2024.I1.012.

[13] Dhivya K, Kalaivani C, Rajambal K. Analysis of Dual Terminal Inverter Topologies. In2018 4th International Conference on Electrical Energy Systems (ICEES) 2018 Feb 7 (pp. 32-37). IEEE. https://doi.org/10.1109/ICEES.2018.8442375

[14] Merlin MM, Green TC, Mitcheson PD, Trainer DR, Critchley DR, Crookes RW. A new hybrid multi-level voltage-source converter with DC fault blocking capability. In9th IET international conference on AC and DC power transmission (ACDC 2010) 2010 Oct 19 (p. O56). Stevenage UK: IET. https://doi.org/10.1049/cp.2010.0987

[15] Rama ST, Rajini V. Mathematical Model of Alternate Arm Converter. InICDSMLA 2020: Proceedings of the 2nd International Conference on Data Science, Machine Learning and Applications 2021 Nov 9 (pp. 1479-1495). Singapore: Springer Singapore. https://doi.org/10.1007/978-981-16-3690-5_141

[16] Tian Y, Wickramasinghe HR, Li Z, Pou J, Konstantinou G. Review, classification and loss comparison of modular multilevel converter submodules for HVDC applications. Energies. 2022 Mar 9;15(6):1985. https://doi.org/10.3390/en15061985.

[17] Merlin MM, Green TC. Cell capacitor sizing in multilevel converters: cases of the modular multilevel converter and alternate arm converter. IET Power Electronics. 2015 Mar;8(3):350-60. https://doi.org/10.1049/iet-pel.2014.0328

[18] Gao C, Yang J, He Z, Tang G, Zhang J, Li T, He D. Novel controllable-line-commutated converter for eliminating commutation failures of LCC-HVDC system. IEEE Transactions on Power Delivery. 2022 Jun 16;38(1):255-67. https://doi.org/10.1109/TPWRD.2022.3183599

[19] Rajan P, Jeevananthan S. Toward Energy Sustainability—Domestic Power Station, Tariff Acquiescent EMS, and Procedure to Rejuvenate Petrol Scooter Into Electric Scooter for Accelerated Participation of Rural

Consumers in Energy Demand Management. IEEE Journal of Emerging and Selected Topics in Power Electronics. 2022 Jun 13;11(4):4442-52. https://doi.org/10.1109/JESTPE.2022.3182574

[20] Lenine D, Reddy N. Design and Performance Analysis of Magnetic Coupled Trans Impedance Inverter. In2024 International Conference on Distributed Computing and Optimization Techniques (ICDCOT) 2024 Mar 15 (pp. 1-6). IEEE. https://doi.org/10.1109/ICDCOT61034.2024.10516030

[21] Reddy MM, Varma PS, Lenine D. Improving gain of real time PI controller using particle swarm optimization in active power filter. Microprocessors and Microsystems. 2023 Mar 1;97:104760. https://doi.org/10.1016/j.micpro.2023.104760

[22] Priyanka G, Kumari JS, Lenine D, Varma PS, Madhuri SS, Chandu V. MATLAB-Simulink environment based power quality improvement in photovoltaic system using multilevel inverter. Electrical Engineering & Electromechanics. 2023 Mar 5(2):43-8. https://doi.org/10.20998/2074-272X.2023.2.07.

[23] Farr EM, Feldman R, Watson AJ, Burgos RP, Clare JC, Wheeler PW, Boroyevich D. Alternate Arm Converter (AAC) operation under faulted AC-grid conditions. In7th IET international conference on power electronics, machines and drives (PEMD 2014) 2014 Apr 8 (pp. 1-6). IET. https://doi.org/10.1049/cp.2014.0358